Polarization-selective resonant photonic crystal photodetector

Jin-Kyu Yang,[1,a)] Min-Kyo Seo,[1] In-Kag Hwang,[2] Sung-Bock Kim,[3] and Yong-Hee Lee[1]
[1]*Department of Physics, Korea Advanced Institute of Science and Technology, Daejeon 305-701, Republic of Korea*
[2]*Department of Physics, Chonnam National University, Gwangju 500-757, Republic of Korea*
[3]*Telecommunication Basic Research Laboratory, Electronics and Telecommunications Research Institute, Daejeon 305-600, Republic of Korea*

(Received 7 October 2008; accepted 6 November 2008; published online 25 November 2008)

Resonance-assisted photonic crystal (PhC) slab photodetectors are demonstrated by utilizing six 7-nm-thick InGaAsP quantum wells. In order to encourage efficient photon coupling into the slab from the vertical direction, a coupled-dipole-cavity-array PhC structure is employed. Inheriting the characteristics of the dipole mode, this resonant detector is highly polarization selective and shows a 22-nm-wide spectral width. The maximum responsivity of 0.28 A/W, which is >20 times larger than that of the identical detector without the pattern, is observed near 1.56 μm. © *2008 American Institute of Physics*. [DOI: 10.1063/1.3036954]

Many researchers have tried to control light using two dimensional slab photonic crystal (PhC) structures, taking advantage of the possibility of photon confinement by photonic band gap and total internal reflection. In recent years, electrically pumped PhC lasers,[1] microfluidic PhC waveguide sensors,[2] ultra small PhC filters,[3] and high-efficiency PhC light emitting diodes[4] have been continuously reported. Note that most of these researches were focused on emission and propagation of light, rather than absorption. It was recently reported that the threshold of a PhC laser could be decreased by utilizing resonant absorption near PhC band edge where the photonic density of states is high.[5] High-efficiency midinfrared photon detection was also demonstrated by employing PhC structures,[6] where the introduction of a PhC structure with an InAs/InGaAs/GaAs quantum dot increased the photon conversion efficiency and reduced the signal-to-noise ratio. It is worth pointing out that the incorporation of a specific PhC resonance with the detector increases the effective absorption length. Moreover, the finite bandwidth of the resonance naturally provides spectral-filtering capability to this photodetector. However, in the case of infrared PhC detectors, it has been nontrivial to realize resonant-enhanced PhC detectors with high quality factors because of the weak index contrast in the vertical direction.

Here, we investigate the possibility of efficient photon detection using a high-contrast PhC thin slab structure containing InGaAsP/InP multiple quantum wells (QWs) near an optical communication region. In order to increase the effective absorption length of the thin QW, the high-quality-factor resonant cavity is employed in the form of an array.[7] In addition, we modified the PhC cavity structure for the better coupling between the incoming light and the cavity mode.

Efficient vertical coupling between incident photons and a PhC mode is one of the basic requirements for photodetectors having a very thin absorption layer. However, in general, it is not straightforward to couple normally incident light to a PhC mode, which needs to satisfy the symmetry match requirements.[8] Here, we plan to employ the doubly degenerate dipole mode in a single-cell PhC cavity for photodetection. This dipole mode promises inherent vertical radiation and has intensity maxima near the cavity center.[9] In this paper, we propose and demonstrate the coupled-cavity-array (CCA) PhC structure for resonant photon detection over a large area.

The optimized CCA PhC structure is obtained by the finite-difference time-domain (FDTD) method, as shown in the inset of Fig. 1(a). To increase the quality factor, four nearest air holes are reduced and pushed out from the center.[10] When the radius of modified air holes is 0.3a, the quality factor is largest. Figures 1(b) and 1(c) show the field intensity distributions of the resonant dipolelike array mode on a logarithmic scale. Note that the photons are localized at the center of the slab and are emitted from the slab like a

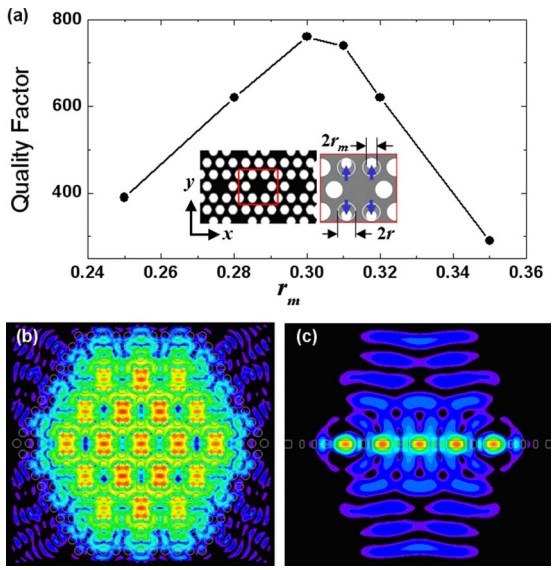

FIG. 1. (Color online) Design of the CCA PhC structure. (a) Optimization of the CCA structure by modifying nearest air holes as shown in the inset, and field intensity distributions of the resonant dipolelike array mode on a logarithmic scale (b) along the horizontal cross section of the slab and (c) along the vertical cross section of the slab when quality factor is maximized at r_m=0.3a. Here, the thickness of the slab is 0.6a, and the radius of initial air holes (r) is 0.35a, respectively, where a is the lattice constant of PhC.

[a)]Author to whom correspondence should be addressed. Electronic mail: jin9ya@gmail.com. Present address: Department of Applied Physics, Yale University, New Haven, CT 06520-8284.

 © 2008 American Institute of Physics

Author complimentary copy. Redistribution subject to AIP license or copyright, see http://apl.aip.org/apl/copyright.jsp

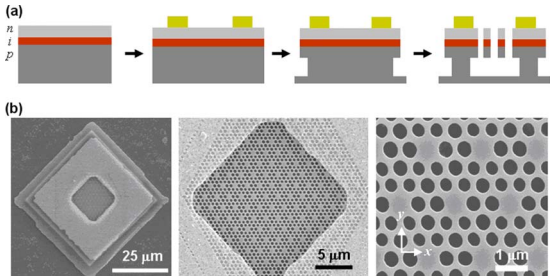

FIG. 2. (Color online) Fabrication of the CCA PhC detector. (a) Schematic view of fabrication (simple structure of *n-i-p* doped InGaAsP/InP QWs, *n*-electrode formation, mesa construction, and PhC pattern introduction in sequence) and (b) SEM images of a fabricated sample with different magnifications.

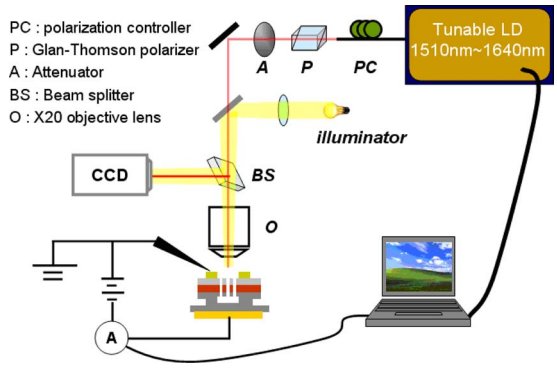

FIG. 3. (Color online) Photocurrent measurement setup.

plane wave. Because of the anisotropic modification, the degeneracy of two dipolelike modes is broken and split into two modes of different resonant frequencies.

We used six 7-nm-thick InGaAsP multiple QWs for the PhC photodiode surrounded by heavily doped InGaAsP layers. The doping densities of top n and bottom p layers are $\sim 2.7\times 10^{19}/\mathrm{cm}^3$ and $\sim 2.5\times 10^{18}/\mathrm{cm}^3$, respectively. The fabrication procedure shown in Fig. 2(a) is composed of two steps: the formation of a mesa and the fabrication of PhC patterns. In order to prevent the photocurrent leakage, the mesa structure is electrically isolated.

At first, the photoresist (PR) pattern for the electrode is prepared by photolithography. Then, a ring-shaped AuGe electrode is formed by thermal evaporation and lift-off. To protect the surface of the wafer from subsequent processes, a thin Si_xN_y buffer layer is coated by plasma enhanced chemical vapor deposition. Next, the PR pattern for the mesa structure including the electrode is prepared by second photolithography. The pattern is transferred into a p-InP sacrificial layer by the chemically assisted ion-beam etching (CAIBE). After wet etching by a diluted HCl solution at room temperature, the slightly undercut mesa structure is formed. Finally, PR remnants and protection layer are removed in sequence by O_2 ashing and buffered oxide etch solution.

The second procedure is the formation of freestanding PhC slabs supported by the pedestal underneath the electrode. The polymethyl methacrylate (PMMA) is coated by a spin coater, and then the PhC pattern is generated on the PMMA by the electron-beam lithography. In this process, the PhC pattern is carefully aligned with the inner region of the ring-shaped electrode. After the PMMA hardening by Ar ion bombardment, the PhC pattern is transferred into the sacrificial layer by CAIBE. Finally, after removing the residual PMMA, the second wet etching is performed at low temperature (4 °C) for constructing the freestanding PhC slab to form the post just underneath the electrode. Figure 2(b) shows a scanning electron microscope (SEM) image of the fabricated sample. The lattice constant is 540 nm. The radii of the regular and modified air holes are $0.372a$ and $0.344a$, respectively. The slab thickness is 282.5 nm, including six 7-nm-thick QWs.

Polarization-dependent photocurrent spectra are measured by using a tunable laser diode and a picoampere meter, as shown in Fig. 3. The wavelength of the laser diode is varied from 1510 to 1640 nm. The incident polarization state is controlled by a polarization controller and a Glan-Thomson polarizer. The input beam is focused on the PhC pattern by a microscope objective lens (numerical aperture of 0.24). To supply a bias voltage and measure photocurrents, a microcontact tungsten tip on the electrode is employed. The photocurrent signal from the picoampere current meter is synchronized to the tunable diode laser. To reduce noises, the tip is directly bonded to a BNC cable.

Polarization-selective photocurrent spectra for 16-μm-wide squares are measured at room temperature and plotted in Figs. 4(a) and 4(b). The detector is biased at a voltage of −12 mV, where the maximum response is observed. The optical power of the incident light is 2 μW. All photocurrent spectra are registered after subtracting the background (dark) current. According to the photocurrent spectra without a PhC pattern (the gray in the graphs), the QW absorption coefficient is assumed to be 7000 cm^{-1} near 1.53 μm,[11] which corresponds to less than 3% absorption considering a single pass though seven QWs employed in the experiment.

Polarization-dependent enhancement is observed in the photocurrent spectra near the dipole resonance wavelength. As shown in Fig. 4(a), the photocurrent is resonantly enhanced at 1.63 μm with an 8-nm bandwidth for x-polarized light. In the spectral region outside of this dipole resonance, the responsivity of the PhC sample is lower than that of the bulk sample because of the reduction in the QW area. The maximum responsivity of 0.28 A/W is observed for y-polarized light at 1.56 μm, where the measured photocurrent is 0.567 μA with incident optical power of 2 μW [Fig.

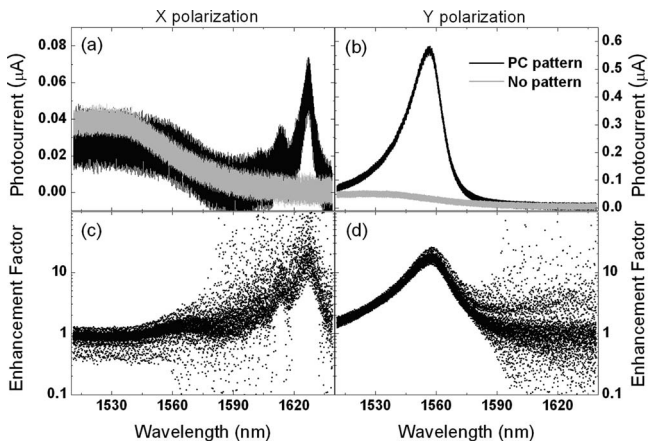

FIG. 4. Spectral photocurrent responses and enhancement of photocurrent with and without PhC patterns: [(a) and (c)] for x-polarized light and [(b) and (d)] for y-polarized light. All photocurrent spectra are plotted after subtracting the background (dark) current.

Author complimentary copy. Redistribution subject to AIP license or copyright, see http://apl.aip.org/apl/copyright.jsp

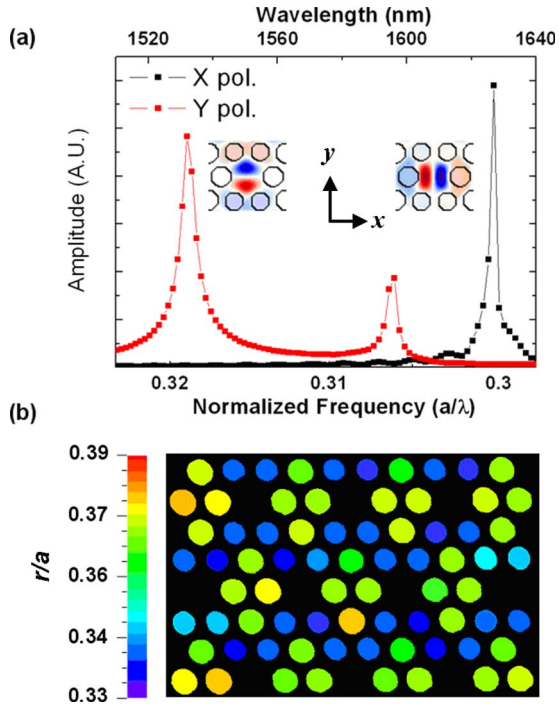

FIG. 5. (Color online) (a) Coupled modes at the CCA PhC slab from the normal incident plane wave calculated by the periodic FDTD method. (b) Magnified SEM image near the center of the sample. The air hole size is represented by colors, indicated in the color bar to the left.

4(c)]. The spectral full width at half-width of this detector is 22 nm. This detector response corresponds to the quantum efficiency (η) of 22.5%,[12]

$$\eta = (i_c h\nu_p / ep).$$

Here, i_c is the photocurrent, ν_p is the frequency of incident light, and P is the incident optical power. The enhancement factor of the photocurrent is defined with respect to the reference sample without pattern. According the measurement shown in Figs. 4(b) and 4(d), the enhancement factors are >20 near resonant wavelengths, in spite of the carrier leakage and reduced absorbing area.

To understand the resonant photocurrent enhancement of PhC photodiodes, FDTD methods are used. In the calculation, the supercell method is employed to describe the infinitely repeating CCA PhC structure. From the SEM image, the lattice constant in the x-direction (a_x) and y-direction (a_y) are estimated to be 528 and 551 nm, respectively. The radii of the air hole and the modified air hole are 203 and 180 nm, respectively. The slab thickness is 282.5 nm, and the index of the slab is assumed to be 3.4. As shown in Fig. 5(a), three resonant peaks are found in the experimental range from 1510 to 1640 nm. The x-dipole-like mode appears at 1630 nm with a quality factor of 2700. On the other hand, because of the nonsymmetric perturbation, the y-dipole-like mode is found near 1530 nm with a relatively low quality factor of 520. The resonance near 1600 nm is a TM-like mode in which the intensity minimum is located at the center of the slab. These results agree well with experimental data except the small blueshift of the y-dipole-like resonance. The mismatches originate from the imperfectly fabricated sample, where one unit cell of the fabricated structure is not identical to the next unit cell. In order to check the fabrication imperfection, we digitized the SEM image of Fig. 2(b) and represented the variation in air hole size by artificial colors, as shown in Fig. 5(b). According to the SEM image, the maximum variation in air hole size is about 5%. We believe that the higher quality factor and efficiency can be realized from better fabricated samples.

In summary, polarization-selective resonant photodetectors are proposed and demonstrated by the CCA PhC slab structure. In this structure, the dipolelike array mode shows good vertical coupling characteristics. We achieved maximum responsivity about 0.28 A/W near the dipole resonance at 1.56 μm by utilizing six 7 nm InGaAsP QWs, which corresponds to over 20-fold enhancement in comparison to the identical sample without patterns. We expect that the resonant-assisted PhC photodetection scheme can realize a new optical device such as the multichannel converter from optical signal to electrical signal.

This work was supported by the Korea Science and Engineering Foundation (KOSEF) (No. ROA-2006-000-10236-0) and KOSEF S&T graduate scholarship.

[1] H.-G. Park, S.-H. Kim, S.-H. Kwon, Y.-G. Ju, J.-K. Yang, J.-H. Baek, S.-B. Kim, and Y.-H. Lee, Science **305**, 1444 (2004).
[2] M. Lončar, B. G. Lee, L. Diehl, M. A. Belkin, F. Capasso, M. Giovannini, J. Faist, and E. Gini, Opt. Express **15**, 4499 (2007).
[3] B. S. Song, S. Noda, and T. Asano, Science **300**, 1537 (2003).
[4] S.-K. Kim, H. K. Cho, D. K. Bae, J. S. Lee, H.-G. Park, and Y.-H. Lee, Appl. Phys. Lett. **92**, 241118 (2008).
[5] F. Raineri, G. Vecchi, C. Cojocaru, A. M. Yacomotti, C. Seassal, X. Letartre, P. Viktorovitch, R. Raj, and A. Levenson, Appl. Phys. Lett. **86**, 091111 (2005).
[6] K. T. Posani, V. Tripathi, S. Annamalai, N. R. Weisse-Bernstein, S. Krishna, R. Perahia, O. Crisafulli, and O. J. Painter, Appl. Phys. Lett. **88**, 151104 (2006).
[7] H. Altug and J. Vuckovic, Opt. Express **13**, 8819 (2005).
[8] S.-H. Kwon and Y.-H. Lee, IEICE Trans. Electron. **E87**, 308 (2004).
[9] O. Painter, J. Vuckovic, and A. Scherer, J. Opt. Soc. Am. B **16**, 275 (1999).
[10] M. Lončar, M. Hochberg, A. Scherer, and Y. Qiu, Opt. Lett. **29**, 721 (2004).
[11] When the photons pass through the photodiode, the quantum efficiency η is defined as $\eta=(1-R)\cdot(1-e^{-\alpha d})=(i_c h\nu_p/eP)$ if the additional carrier leakage is negligible. Here, R is a reflectivity at the top surface of the diode, α is the absorption coefficient, d is the thickness of the active layer, i_c is the photocurrent, ν_p is the frequency of the incident light, and P is the incident optical power.
[12] A. Yariv, *Optical Electronics in Modern Communications* (Oxford University Press, New York, 1997).

Author complimentary copy. Redistribution subject to AIP license or copyright, see http://apl.aip.org/apl/copyright.jsp